

# CHIMTEA—Chemical Impact of Thunderstorms on Earth’s Atmosphere

Enrico Arnone and Bianca Maria Dinelli

**Abstract** Since their accidental discovery in the 1990s, lightning-related sprites, other transient luminous events (TLEs), and terrestrial gamma-ray flashes have shown us how the impact of thunderstorms extends from the troposphere up to the upper atmosphere and ionosphere. Thunderstorms are a key player for the climate system, in particular through lightning-produced  $\text{NO}_x$  and troposphere–stratosphere exchange. The Chemical Impact of Thunderstorms on Earth’s Atmosphere (CHIMTEA) project focused on TLE-producing thunderstorms and their possible impact on stratospheric  $\text{NO}_x$  and ozone. The distribution and seasonal cycle of thunderstorm activity were studied through global lightning data and TLE observations over Europe. Michelson Interferometer for Passive Atmosphere Sounding (MIPAS)/Environmental Satellite (ENVISAT) measurements of  $\text{NO}_x$ , ozone, and other related constituents from the upper troposphere to the mesosphere were analyzed with a 2D tomographic approach to quantify thunderstorm-induced changes and explore how to improve their detectability. The study included observations from Global Ozone Monitoring by Occultation of Stars (GOMOS)/ENVISAT, other satellites, and in situ measurements. The sensitivity of the measurements to sprite- $\text{NO}_x$  was investigated through ad hoc radiative transfer simulations quantifying reference thresholds. Global and regional observations showed sprite- $\text{NO}_x$  to be at the edge of current detectability, with no detectable impact on ozone. Model simulations were performed including for the first time a sprite- $\text{NO}_x$  parameterization in the Whole Atmosphere Community Climate Model (WACCM): it was shown that sprites may contribute significantly to tropical  $\text{NO}_x$  in the middle mesosphere and reach detectable levels above particularly active thunderstorms. Extension of the adopted strategy to study lightning- $\text{NO}_x$  was recommended, whereas the modeling and multi-satellite approach was shown to be suitable in support to the upcoming space missions.

---

E. Arnone (✉) · B.M. Dinelli  
Istituto di Scienze dell’Atmosfera e del Clima ISAC-CNR, Bologna, Italy  
e-mail: e.arnone@isac.cnr.it

# 1 Introduction

Clouds are a core component of the Earth's climate system and one of the key shortages in our understanding of a changing climate (IPCC, 2013, [www.ipcc.ch](http://www.ipcc.ch)). Thunderclouds, in particular, affect the dynamics and chemistry of the atmosphere through convective transport and electrification processes. Beside their severe action at the surface, they impact the interface between the troposphere and the stratosphere, one of the most delicate regions of coupling between chemistry and climate, both dynamically and through lightning-produced  $\text{NO}_x$ . The detection of upper atmosphere lightning and gamma energy emissions from thunderstorms has further highlighted the relevance of thunderstorms also at higher altitude.

## 1.1 *Lightning in the Upper Atmosphere*

Since the 1990s, a whole family of upper atmosphere electrical processes have been discovered to occur above thunderstorms: they are known as transient luminous events (TLEs) in their optical and low energy manifestation, and terrestrial gamma-ray emissions (TGFs) in their high energy component (e.g., [18, 19]). In particular, TLEs are produced by the electrical impact of thunderstorms on the above atmosphere, which causes ionization, dissociation, and excitation of neutral air constituents and the consequent well-recognizable optical emissions. They occur in the stratosphere–mesosphere between the top of thunderclouds and the lower ionosphere, the altitude of occurrence determining both their nature and the impact they exert. Above thunderclouds, the formation of streamers (weakly ionized plasma channels) can occur roughly up to 70 km altitude, above which dielectric relaxation timescales become comparable with that of dissociative attachment, leading to diffuse emissions (e.g., [19]). TLEs such as blue jets and gigantic jets are streamer–leader processes injected from thundercloud tops toward the ionosphere and may be considered the upward equivalent of cloud-to-ground (CG) lightning [16]. Sprites [23] are luminous discharges that initiate at about 70–80 km altitude, extend downward to 40 km as streamers and upward to 90 km altitude as diffuse emission, at times in the form of a halo, and are tens of kilometers wide. Elves are diffuse emission rings manifesting the impact of the electromagnetic pulse propagated from a CG on the lower edge of the ionosphere (e.g. [19]). Depending on the relaxation timescales at the altitude of occurrence, TLEs last a few to a few hundred milliseconds. Their continuous occurrence around the globe makes them however a relevant and as yet not considered component of the atmosphere.

## 1.2 *Chemistry of Thunderstorms and Transient Luminous Events*

In the upper troposphere, lightning is a dominant source of active nitrogen oxides  $\text{NO}_x$  ( $\text{N} + \text{NO} + \text{NO}_2$ ), which may consequently be transported into the lower stratosphere with tropospheric pollutants by the slow meridional circulation or by deep convection (e.g., [22]). This source contributes to the main production of  $\text{NO}_x$  by oxidation of tropospheric  $\text{N}_2\text{O}$ , and therefore to catalytic cycles affecting ozone (e.g., [9]). Despite several lightning- $\text{NO}_x$  estimates, observation of lightning  $\text{NO}_x$ , and in particular of its transport into the stratosphere, remains a challenge for current satellites: this is due to a limited sensitivity to upper troposphere  $\text{NO}_x$  species both for limb sounders (efficient in the stratosphere) and nadir sounders (strongly weighted by the tropospheric component), and the relatively small size of individual events. Further limitations arise from the reconversion of lightning- $\text{NO}_x$  into  $\text{HNO}_3$  with consequent loss through scavenging, from high dynamical variability of the upper troposphere–lower stratosphere region, and from the large variability among thunderstorm events [8, 22].

In analogy to tropospheric lightning, TLEs were predicted to impact the atmospheric chemistry. Enell et al. [13], Sentman et al. [24], Gordillo-Vazquez [14], and Winkler and Notholt [25] estimated sprite-induced  $\text{NO}_x$  enhancements within sprite streamers between a few to a few hundreds of percent, with negligible ozone changes. Hiraki et al. [15] estimated orders of magnitude increases in  $\text{NO}_x$  and significant ozone changes. Two observational studies investigated sprite-induced perturbations with satellite measurements. Arnone et al. [5–7] found a possible sprite-induced  $\text{NO}_2$  perturbation of 10 % at 52 km altitude and of tens of percent at 60 km altitude in coincidence of active thunderstorms, and no evident sprite global impact. Rodger et al. [21] concluded that TLEs occurring below 70 km altitude exert no significant impact on the neutral chemistry at a global scale. An impact at local scale but negligible at global scale was also suggested by the first laboratory experiments conducted by Peterson et al. [20], although they were criticized for the poor similarity to real TLE conditions.

This paper presents an overview of the CHIMTEA project, which was developed using several datasets (Sect. 2), to improve our understanding of lightning processes in the upper atmosphere (Sect. 3), and investigate the current sensitivity of observations (Sect. 4) and models (Sect. 5) to describe their chemical impact. Concluding remarks and recommendations from the project are given (Sect. 6).

## 2 Instruments and Data

We used lightning data from several sources: World Wide Lightning Location Network (WWLLN), lightning imaging sensor (LIS), and the VLF/LF lightning detection network (LINET). WWLLN is an experimental global lightning very

low-frequency (VLF) network (<http://www.wvlln.com>) with detection efficiency of about 10 % for CGs and 5 % for intracloud (IC) lightning. Climatological lightning data from the optical transient detector (OTD)/LIS satellite instruments [11] was used for the analysis of observations and model simulations (<http://thunder.msfc.nasa.gov>). LINET data was available at ISAC: it works in the VLF/LF (low-frequency) range with 3D capability and allows for unprecedented low-amplitude detection power, discerning between CG and IC (<http://www.pa.op.dlr.de/linet>). TLE data were collected with tens of low-light sensitive cameras around Europe by the *EuroSprite* network ([18], <http://www.electricstorms.net>). Observations are optical images, which define the “truth” for TLE measurements, and additional radio and infrasound data. The first database of European TLEs was created within CHIMTEA ([2], ACP, *under submission*).

Atmospheric limb observations of the stratosphere–mesosphere (6–70 km altitude) were adopted from the MIPAS2D database [12], obtained from MIPAS/ENVISAT mid-infrared spectroscopic measurements retrieved with the geo-fit multitarget retrieval (GMTR) 2D tomographic code [10]. The 2D approach enables to model horizontal atmospheric inhomogeneities. MIPAS2D data quality was discussed in Dinelli et al. [12]. Pressure, temperature, and ozone-related species and NO<sub>y</sub> family are covered by MIPAS2D results (see further details in [1, 4]). Data from the stellar occultation spectrometer GOMOS/ENVISAT, from the microwave limb sounder (MLS)/Aura microwave thermal emission limb sounder, from sondes, and from the SMOS satellite were used in addition.

We performed TLE-NO<sub>x</sub> simulations on the WACCM [17], which spans from the Earth’s surface to the thermosphere and includes relevant natural processes: the adopted v.4 has updated chemistry, solar proton events, improved stratospheric warming, gravity waves by convection and fronts, and parameterized lightning-NO<sub>x</sub>. The model was run with specified dynamics, which is controlled by nudging temperature and winds below 60 km to specified observational fields, with nudging strength reduced between 50 and 60 km and free running above 60 km. Simulations were run starting on March 2, 2011, with control simulations run for 60 days, perturbed ones until they converged. Meteorological data from European Center for Medium-Range Weather Forecasting (ECMWF) both ERA-Interim (reanalysis) and from operational processing were used both for comparison and scientific analysis.

### 3 TLE-Producing Thunderstorms

A first climatological study of TLEs over Europe was conducted within CHIMTEA coordinating European observations and releasing the first EuroSprite 2009–2012 summary of TLE observations over Europe and the Mediterranean ([2], *under submission*). The occurrence of both summer and winter thunderstorms makes Europe an ideal region for studies of TLEs under seasonally varying conditions

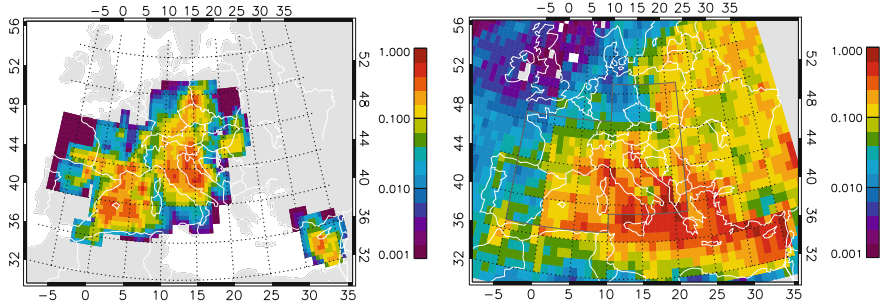


**Fig. 1** *Left* Climatology of observed TLEs (TLEs  $10^{-3} \text{ km}^{-2} \text{ year}^{-1}$ ) for 2009–2012. *Right* Climatology of lightning strokes detected by WWLLN (strokes  $\text{km}^{-2} \text{ year}^{-1}$ ) for 2009–2012. The *grey rectangular shapes* delimit the approximate area of TLE observations used in monthly mean calculations of WWLLN data

and a preferential region for the following chemistry part of the study. Over 2009–2012, the number of optical observations of TLEs exceeded 1000 per year. Because of this unprecedented number of observations, it was possible to construct a climatology of over 6000 TLEs observed above 756 thunderstorms. The number of TLEs per thunderstorm was found to follow a power law, with less than 10 TLEs for 567 thunderstorms and up to 147 TLEs above the most prolific one. The vast majority of TLEs were classified as sprites, 294 as elves, 185 halos, 57 upward lightning, 2 blue jets, and 1 gigantic jet. This number of observed sprites largely exceeds that acquired from satellites over equivalent periods of time. A key shortage of the adopted dataset is the inhomogeneity of the observational coverage. The seasonal changes in the climatology were however extracted weighting each season by the total yearly observations. Figures 1 and 2 report the TLE climatology in terms of geographical distribution and seasonal cycle. For comparison, the same diagrams were replicated with a climatology of lightning data from WWLLN. In the

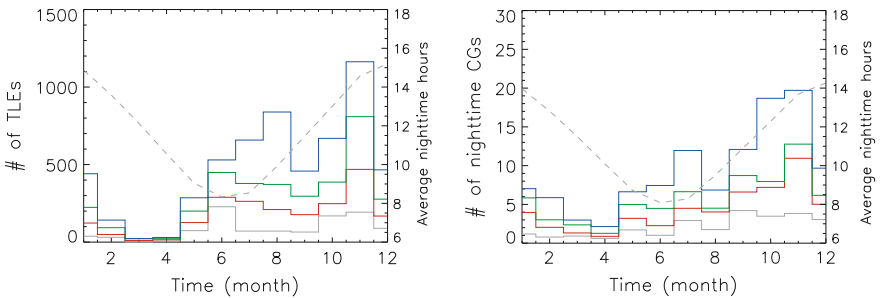


**Fig. 2** Cumulative number of observed TLEs (*left*) and WWLLN CG strokes (*right*) per month including data from the start of the sample (January 2009) to the end of 2009, 2010, 2011 and 2012 (respectively, in *grey, red, green* and *blue*). The average seasonal cycle of nighttime hours is shown (*dashed grey*). WWLLN data are scaled by  $10^4$  and averages calculated over the rectangular shapes shown in Fig. 1

areas covered by the observations, TLE activity in Europe is intense over the Southern regions and Mediterranean Sea. The largest number of TLEs per month is recorded in November, whereas in March and April TLE activity is almost completely halted. This is due to a shift from continental areas in summer to coastal areas and sea in autumn. The peak in November can be reconciled with the number of observations in summer once the change in length of the night is taken into account (see dashed line in the figures), although the larger +CGs/-CGs ratio in autumn/winter maritime thunderstorms should be considered. Elves occur exclusively over autumn/winter maritime thunderstorms. The overall behavior is well consistent among individual years, therefore making the observed seasonal cycle a robust general feature of TLE activity over Europe. The 756 TLE-producing thunderstorms were then used as case studies for several papers and for chemistry-TLE correlations in the next section.

Lightning data from the WWLLN network were used to trace thunderstorm activity. Due to the inhomogeneity of WWLLN detection efficiency, which depends on the distance from the detector, we focused the analysis of WWLLN data over Europe where the available detectors guarantee a satisfactory coverage allowing to study the distribution and seasonal changes of thunderstorm activity. At global scale, WWLLN data were used for correlation with MIPAS measurements (see Sect. 4), assuming WWLLN lightning detections as proxy of thunderstorm rather than individual lightning strokes. Within the regions covered by the observations, the TLE main geographical distribution tends to mimic the distribution of thunderstorm activity, occurring over thunderstorms with an incredible variety of characteristics, from large summer thunderstorms over the continental areas to tiny winter thunderstorms over the sea. This is evident in the northern part of the TLE climatology where large areas with a weak TLE rate are consistent with a drop in lightning activity, e.g., in France and Germany, and partially in Spain contrasting with the adjacent high activity over the Pyrenees. In contrast, the fading of TLE activity in Southern Italy is due to poor coverage. The poor coverage appears to cause similar low rates over Corsica, North-West Italy, and Hungary, where local cameras tend to observe only thunderstorm at a certain distance from the observation spot. Peak TLE rate exceeds  $10^{-3} \text{ km}^{-2} \text{ year}^{-1}$  in a few hotspots in the Balearic Islands, Italy, and Poland, whereas it is typically around 0.2–0.3 in large adjacent regions. This rate should be compared to lightning rates around 0.2–0.3 within the same regions, pointing to a factor of 1000 in the observed lightning/TLE ratio.

Correlation studies between lightning/TLE activity and atmospheric and surface parameters were performed in order to characterize the observed distributions also for parameterization in models. Surface temperature data for continent and sea areas were investigated showing no simplified correlation with lightning over Europe or globally could be found. Soil moisture (SM) and dielectric constant (DC) data measured by the SMOS satellite were also investigated. A correlation was performed in order to seek a possible bias in lightning activity (either in its production or detection by ground networks) consistent with the availability of soil moisture and soil conductivity. The latter may lead to the use of satellite data to improve prediction of thunderstorm occurrence, without relying on standard parameters such

as convective available potential energy and vertical wind shear. Comparison of SM and DC maps with those of lightning activity (not shown) highlighted a strong variability in SMOS data and difficulties in identifying clear patterns which could be reconciled among the different parameters. Averages over the European continent showed a seasonal evolution of SMOS 2011 data for SM and DC imaginary component with a minimum in summer, and maximum in winter, with no reproduction of the seasonal cycle observed in lightning activity. On the contrary, the DC real component averaged over Europe and the Mediterranean Sea showed a seasonal cycle similar to that of lightning activity. However, once the data was limited to the region of EuroSprite coverage, the temporal behavior changed significantly and the possible correlation was largely lost. This lack of consistency showed the complex interplay of different sources of soil moisture, which integrates precipitation from all cloud types and can therefore bury information on convection within its variability. If a correlation exists, this should be further studied adopting a model approach which incorporates all relevant parameters to describe lightning production.

#### 4 Measuring TLE- and Lightning-NO<sub>x</sub> from Space

Comparison of MIPAS2D results with MLS, GOMOS, and ECMWF was performed on key regions and seasons. In particular, GOMOS and MIPAS2D NO<sub>2</sub> showed a fair agreement in the low to mid-latitude stratosphere, supporting the use of MIPAS2D data to study the impact of TLEs in the range of 50–0.2 hPa, with random errors on NO<sub>2</sub> up to 0.7 ppbv at and below 50 km altitude, and around 1–1.3 ppbv at 60 km altitude. A MIPAS2D–GOMOS analysis was performed on the variability of NO<sub>y</sub> in 2002–2012 [1]. A correlation with solar cycle and geomagnetic activity was found at high-latitude stratopause and lower stratosphere, down to mid-latitude. MIPAS2D data under perturbed conditions were also investigated in the extreme 2011 Arctic vortex [4]. At the low to mid-latitude stratopause, NO<sub>2</sub> could be clearly matched to its N<sub>2</sub>O source, tracing the occasional changes due to dynamical year-to-year variability (e.g., during quasi-biennial phases): therefore, a dominant influence of TLE-NO<sub>2</sub> can be excluded and only secondary contributions should be expected.

We performed a series of radiative transfer simulations mimicking TLE-NO<sub>2</sub>. The unperturbed atmosphere was from ECMWF and MIPAS data with 1.125° horizontal and 1 km vertical steps, smoothed and with cloud interferences. Sprite perturbations were applied at various latitudes, at 45–90 km altitude, and over a few hundred kilometers. Figure 3 shows retrieved versus reference NO<sub>2</sub> for perturbations of +1 to +10 ppbv. The simulations at 60 km altitude show 1–2 ppbv biases and oscillations induced by the retrieval. This uncertainty drops to below 1 ppbv when the sprite perturbation occurs over high background. At 52 and 47 km altitude, retrievals pick also at the +1 ppbv perturbation, with a bias of less than 0.5 ppbv. A low altitude TLE scenario was analyzed with perturbations at 15–45 km altitude. The results

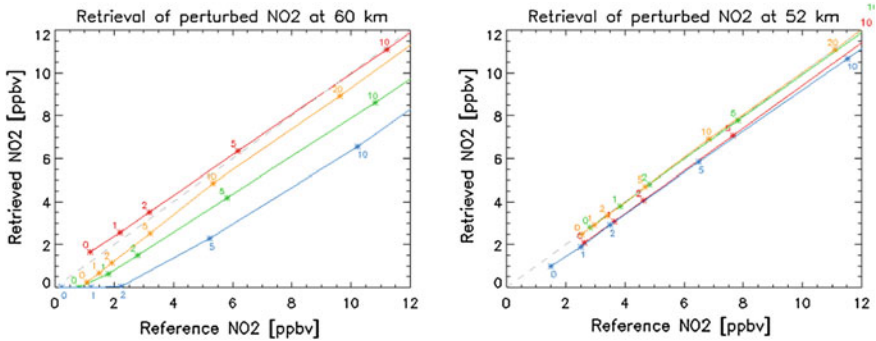


**Fig. 3** Retrieved versus reference  $\text{NO}_2$  for simulations having perturbed  $\text{NO}_2$  at 45–90 km altitude. Results are shown at the location of the three sprite-perturbations (colors are latitude  $32^\circ$  S,  $9^\circ$  S,  $34^\circ$  N, the latter having two perturbed grid points) and at altitude 60 (*left*) and 52 (*right*) km, limited to the low magnitudes (see labels)

show a sensitivity to changes of 0.5 ppbv at 36–42 km, and 1 ppbv at 21–33 km altitude. The 18 km altitude still shows a close-to-linear response to the magnitude of the perturbation, although with larger uncertainties.

We also performed simulations with  $\text{NO}_2$  perturbed at 10–22 km altitude mimicking the effects of lightning or thunderstorm-driven transport. Our simulations show that at 15 km altitude the large amount of  $\text{NO}_2$  retrieved in some orbits is due to artificial oscillations induced by the retrieval. At 18 km altitude, oscillations are typically of the order of 1 ppbv, but can reach 2 ppbv, and drop to 0.5–1.0 ppbv at 21 km, values below which real perturbations cannot be identified. The retrieval greatly improves at low altitude when the validity of the adopted microwindows is artificially extended down to 9 km. In this case, the insensitive level is shifted to the lowermost 9 km altitude, and the other low altitude levels have sensitivity to at least large amounts of  $\text{NO}_2$  (10 ppbv) with sufficient accuracy. When further performing simulations removing clouds, the improvement was substantial in terms of retrieved lightning-perturbed  $\text{NO}_2$  and reduced oscillations. Results of the above simulations showed sensitivity down to 1 ppbv at 60 km, of about 0.5 ppbv at 52 km, and 1–0.5 ppbv at 18–21 km altitudes. Given the presence of background oscillations, this sensitivity can be fully exploited only by averaging a large number of observations in order to reduce the background variability. However, the simulations showed the response of MIPAS  $\text{NO}_2$  measurements to small changes is largely linear once this minimal amounts are reached, so that if enough  $\text{NO}_2$  is already present, MIPAS has sensitivity to smaller perturbations.

#### 4.1 Thunderstorm Signatures in MIPAS2D $\text{NO}_2$

We sought sprite perturbations above thunderstorms correlating MIPAS2D nighttime  $\text{NO}_2$  with WWLLN lightning, extending [6, 7]. This approach allowed us to



have a search at global scale both for TLE effects and other thunderstorm impacts above the upper troposphere. The coincidence window was chosen to be 60 min prior to MIPAS measurement, with horizontal dimensions of 500 km along latitude and 60 km along longitude, and a threshold of 10 WWLLN counts. Results by Arnone et al. [6, 7] over the period August–December 2003 showed a perturbation peak in the thunderstorm-NO<sub>2</sub> of about 1 ppbv (10 %) at 52 km altitude. An extension of this analysis up to April 2004 confirmed a significant change over latitudes 0–20 North (2–5 % at 52 km), with no significant change in ozone or other species. The analysis was extended to the complete dataset of MIPAS mission using MIPAS2D GRD 2.3. Comparison of WWLLN-NO<sub>2</sub> and background NO<sub>2</sub> at various altitude showed no significant perturbation of the distributions (e.g., with anomalous peaks) or a change to the mean or median of the distribution. No significant changes were found in other species. We conclude that there is no robust evidence of thunderstorm-induced effects on the adopted MIPAS2D dataset, and therefore perturbations may be below 0.05 ppbv at 52 km altitude. The adopted statistical method based on global detections of lightning is likely missing a large fraction of the MIPAS coincidences. Moreover, the adopted GRD retrieval method is partly smearing NO<sub>2</sub> perturbations, and most importantly changing the location of the retrieved profile as compared to the original observation. The analysis will need to be repeated with a version of MIPAS2D suited for studying localized changes.

An analysis was performed on chemistry measurements above individual thunderstorms with documented TLE occurrence by the EuroSprite network (see Sect. 3). MIPAS profiles from 2009 to the end of 2011 were inspected in order to find measurements that sounded the atmosphere above the TLE-active thunderstorms. Despite the large number of TLE-producing thunderstorms observed, no robust coincidence was found with MIPAS sounding, with only 24 close matches (i.e., with spatial distances below 100 km and perfect time match). None of the thunderstorm-NO<sub>2</sub> showed a significant change as compared to the background NO<sub>2</sub>. Because of the lack of a perfect match, this search cannot however be conclusive in constraining the NO<sub>2</sub> production by individual TLE-producing thunderstorms.

A further global correlation study was performed with TGF-producing thunderstorms to identify chemical changes induced by high energy emissions or by their low energy tail. The analysis was performed on 11,040 Reuven Ramaty High Energy Solar Spectroscopic Imager (RHESSI) detections in 2002–2011. The coincidence window was  $\pm 3$  h and  $\pm 300$  km, taking into account uncertainty on the geolocation of the TGF footprint and evolution of the thunderstorm. MIPAS NO<sub>2</sub> data at 20–60 km altitude in coincidence with TGF activity showed no consistent enhancement as compared to background NO<sub>2</sub>, therefore pointing to a lack of major regional impact of TGFs on the chemistry of the stratosphere above thunderstorms. A few individual cases of high NO<sub>2</sub> were associated to retrieval of poor data. Small NO<sub>2</sub> changes, or highly localized changes which were missed by MIPAS may not be excluded.

## 5 Climate-Chemistry Sensitivity to TLE-NO<sub>x</sub>

Simulations were performed including for the first time a sprite-NO<sub>x</sub> parameterization in the WACCM [3]. A simplified parameterization of sprite-NO<sub>x</sub> was calculated using vertical profiles from Enell et al.'s [13] ion-neutral chemistry model. Climatological fields of lightning activity from the LIS/OTD [11] were used as a proxy of sprite activity with a rate of 1 sprite every 1,000 lightning flashes (leading to 2–3 sprites/minute globally). The simulations started at magnitude 10 and 100 times the reference sprite-NO<sub>x</sub> climatology to produce a sprite-NO<sub>x</sub> dominated scenario, followed by lower magnitude perturbations, both constant in time and with a switch-off after 20 days.

Investigation of the climate-chemistry sensitivity of the atmosphere to sprite-like perturbations was performed at varying magnitude, time, and space constraints, allowing the quantification of a threshold for reaching significant changes. Results for the 10x case study are shown in Fig. 4 (with red indicating peak values of 2 ppbv, or about 400 % increase). Horizontal plumes of enhanced NO<sub>x</sub> originating above the Americas, Central Africa, and the Maritime Continent buildup and expand to cover much of the tropics. Over the 40 days of the simulation, the enhanced NO<sub>x</sub> fills regions of very low background NO<sub>x</sub>. Tongues of downward transported NO<sub>x</sub> can interfere with the sprite-NO<sub>x</sub> perturbation at Northern latitudes. Peak values of up to a factor 4 (a factor 20 in the x100 case) enhancement are reached within a couple of weeks above Africa and up to a factor 3 (a factor 10 in the x100 case) above the Maritime Continent, at 66–80 km altitude, down to tens of percent at 60 km. Results for the simulations with the reference 1x perturbation at

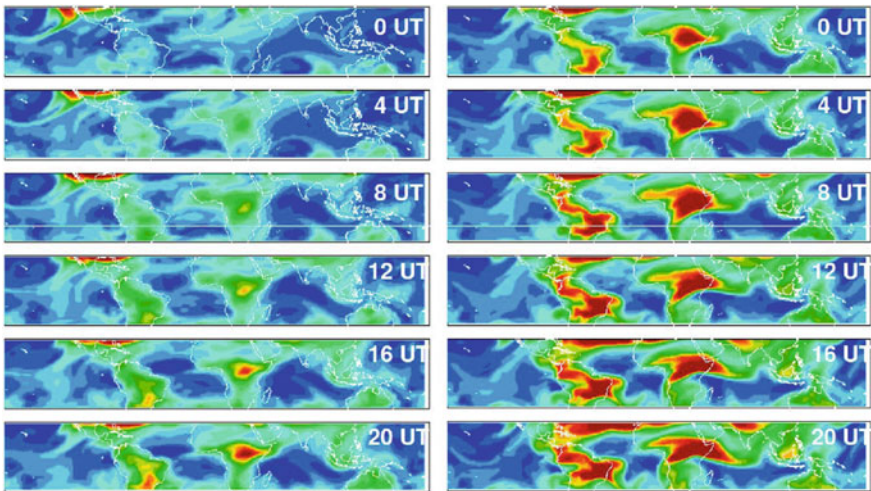


**Fig. 4** WACCM response to sprite-NO<sub>x</sub> (x10) at 70 km altitude during day 1 (*left column*) and day 2 (*right column*) of the perturbations, at 4 h time intervals

0.05 hPa (about 70 km) are shown in Fig. 5 as difference between the perturbed (dashed lines) and control simulations. The difference to the control run is significant, and saturates within the tropics at about +0.2 ppbv of  $\text{NO}_x$  more than the control simulation. Note that the variability of the tropical averaged  $\text{NO}_x$  is around  $\pm 0.02$  ppbv. The saturation of the sprite- $\text{NO}_x$  source is reached in about 15 days. Oscillations in the timeseries are due to air masses moving in and out of the averaging box region, and  $\text{NO}_x$  responses building up differently depending on the specific background conditions. The enhancement is also seen in the zonal mean values at the tropics (black line), with a smoother steady increase. A test whereby the sprite- $\text{NO}_x$  source is ramped down after 20 days (bold lines) shows that the atmosphere relaxes back to background conditions in about 15 days, i.e., similarly as for the buildup time.

The results show that, without consideration of the competition of transport and sinks, previous attempts to estimate the relevance of sprite- $\text{NO}_x$  to the atmosphere at regional or global level are unreliable since the atmosphere needs to reach equilibrium with the sprite source. Our simulations point to a 0.2 ppbv (about 30 %) contribution to Tropical  $\text{NO}_x$  at 70 km altitude by sprites assuming [13] maximum case (our reference scenario), down to 0.02 ppbv buried within background variability assuming the larger of their typical case. This is above the variability we found for Tropical  $\text{NO}_x$  at 70 km altitude (about 0.01 ppbv). Below these values the sprite contribution to Tropical  $\text{NO}_x$  becomes irrelevant. The relaxation timescales for Tropical  $\text{NO}_x$  at 70 km altitude are of the order of 15 days, so that global effects of sprite- $\text{NO}_x$  will be integrated over such time periods even though they occur impulsively.

We also used model results to interpret available observational studies. Considering periods of maximum buildup under slow transport, we can expect peaks of tens of percent change in  $\text{NO}_x$  at 60–85 km altitude. At this magnitude,

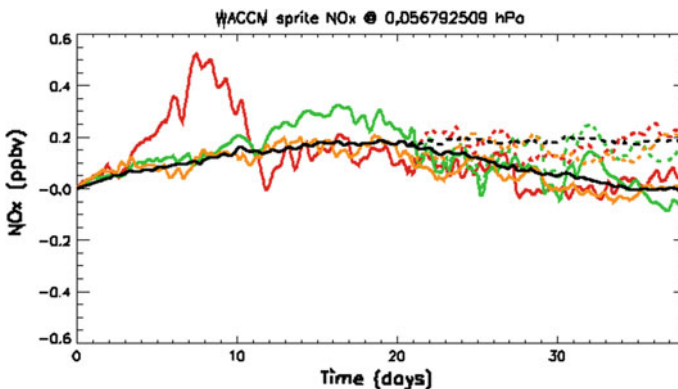


**Fig. 5** WACCM response to sprite- $\text{NO}_x$  perturbations in the case 1x (*bold*) and in the case 1x with rampdown after 20 days (*dashed*). Results are shown as difference between the perturbed and reference simulation above target regions South America (*yellow*), Central Africa (*red*), South East Asia (*green*) and Tropics (*black*)

sprite-NO<sub>x</sub> have detectable levels under favorable conditions. This confirms what is suggested by the analysis of satellite observations of NO<sub>x</sub> by Arnone et al. [6, 7], Rodger et al. [21], and Arnone et al. [5], with significant impact at local scale and negligible at global scale. At this magnitude of perturbation, any impact on the atmosphere would be negligible (see, e.g., [7]). Ad hoc calculations to resemble the method applied by Rodger et al. [21] showed their use of partial column should be limited to 65–80 km altitude in order to have sensitivity to sprite-NO<sub>x</sub>.

At lower altitudes, it is unlikely that a global effect can be reached by low altitude TLEs such as blue jets because of the much larger number density. However, local effects under favorable transport conditions may not be excluded. Future work will consider the impact of the complete TLE family. On the other hand, the results of our study at sprite altitude are valid for any other kind of thunderstorm-induced NO<sub>x</sub> perturbation over the same altitude range, which includes other TLEs, TGFs, or other thunderstorm-induced processes in the lower mesosphere.

## 6 Conclusions and Future Lines

CHIMTEA activities have focused on TLE-producing thunderstorms and their impact on stratospheric NO<sub>x</sub> and ozone. The global distribution of thunderstorm activity was traced using global lightning data. Coordination and analysis of an unprecedented number of *EuroSprite* observations produced the first climatology of TLEs over Europe and several case studies. The coordinated European observations were adopted as ground support by the Japanese JEM-GLIMS mission launched in 2012 and will become a core element in ESA 2016 ASIM mission.

The sensitivity of MIPAS/ENVISAT observations to stratospheric variability was compared to extreme conditions occurring under solar proton events and winter polar vortex. The sensitivity to thunderstorm-perturbed NO<sub>2</sub> at various altitude was investigated with radiative transfer simulations finding minimum thresholds of 1 ppbv at 60 km altitude, 0.5 ppbv at 52 km and in the range 18–21 km. These thresholds make it largely unfeasible to use MIPAS for robust lightning-NO<sub>x</sub> detection. Despite the large MIPAS2D dataset and a significant number of thunderstorms with detected TLE or TGF activity, no robust evidence for thunderstorm-perturbed NO<sub>x</sub> was found. Global and regional observations showed sprite-NO<sub>x</sub> to be at the edge of current detectability, with no detectable impact on ozone. Strategies for improving sprite-NO<sub>x</sub> detectability include the use of refinements in the adopted retrieval and satellite measurements having higher spatial resolution.

Simulations were performed including for the first time a sprite-NO<sub>x</sub> parameterization in a global circulation model. Investigation of the climate-chemistry sensitivity to sprite-like perturbations was performed at varying magnitude, time, and space constraints, allowing the quantification of a threshold for reaching significant changes. On the basis of the current knowledge of sprite chemistry, it was

shown that sprites may be able to contribute significantly to tropical  $\text{NO}_x$  in the middle mesosphere, with a spread component up to 0.2 ppbv (30 %) at 70 km altitude, and may reach detectable levels above particularly active thunderstorms. TLE perturbations are therefore likely to have an atmospheric impact, although at or below the edge of current observational capabilities. A key issue is being able to find a perfect match between TLE activity and chemistry measurements, which has to date been missed. Extension of the adopted strategies to study lightning- $\text{NO}_x$  is recommended, whereas the modeling and multi-satellite approach was shown to be suitable in support to the upcoming space missions.

**Acknowledgements** E. Arnone is pleased to acknowledge collaborations: MIPAS2D with Dinelli, Castelli, ISAC-CNR, Papandrea, Carlotti, Univ. Bologna, Italy; WACCM with Smith (NCAR, CO, US), Kero, Enell (SGO, Finland); GOMOS with Hauchecorne, LATMOS, France; MLS by NASA. Thank ECMWF for their data. Lightning data provided and discussed with: LINET (Dietrich, Mugnai, Formenton, ISAC), EUCLID (via EuroSprite), WWLLN (Kero, SGO), LIS (NASA). MIPAS2D-lightning correlation by Kero (SGO). Cloud observations from Meteosat, with Sao Sabbas (INPE, Brazil), Soula (Obs. Midi-Pyrénées, France), Laviola (ISAC). SMOS data from Montzka and Rötzer (Forschungszentrum Jülich, Germany). TLE data from EuroSprite (<http://www.electricstorms.net>) with Neubert, Chanrion (DTU Space, Denmark), van der Velde (Univ. Politècnica de Catalunya, Spain), Soula (Obs. Midi Pyrénées, France), Bor (Geodetic Geophys. Res. Inst., Sopron, Hungary), Haldoupis (Univ. Crete, Greece). TLE data over Italy from the Italian Meteor and TLE Network (IMTN). TLE camera at ISAC observatory on Mt. Cimone with Prevedelli (Univ. Bologna) and support by Bonasoni and group (ISAC) and IMTN (Italy). RHESSI data with Gjesteland (Univ. Bergen, Norway). Support by ESA through funding, feedback by ESA contact Fehr, CESN coordination by Sabia and Fernandez, access to ESA data. Support by ISAC, through funding, hosting, and access to facilities and expertise.

## References

1. Arnone E, Hauchecorne A (2012) Stratosphere  $\text{NO}_y$  species measured by MIPAS and GOMOS onboard ENVISAT during 2002–2010: Influence of plasma processes onto the observed distribution and variability. *Space Sci Rev* 168:315–332
2. Arnone E et al (2015) On the distribution and seasonal cycle of transient luminous events over Europe and the Mediterranean Sea. To be submitted to *ACP*
3. Arnone E et al (2014) WACCM climate chemistry sensitivity to sprite perturbations. *J Geophys Res* 119(11):6958–6970
4. Arnone E et al (2012) Extreme ozone depletion in the 2010–2011 Arctic winter stratosphere as observed by MIPAS/ENVISAT using a 2-D tomographic approach. *Atmos Chem Phys* 12(19):9149–9165
5. Arnone E et al (2009) Seeking sprite-induced signatures in remotely sensed middle atmosphere  $\text{NO}_2$ : latitude and time variations. *Plasma Sources Sci Technol* 18:1–10
6. Arnone E et al (2008) An estimate of the impact of transient luminous events on the atmospheric temperature. *Advances in Geosc.* 13(13):37–43
7. Arnone E et al (2008) Seeking sprite-induced signatures in remotely sensed middle atmosphere  $\text{NO}_2$ . *Geophys Res Lett* 35:L05807
8. Beirle S et al (2010) Direct satellite observation of lightning-produced  $\text{NO}_x$ . *Atmos Chem Phys* 10:10965–10986. doi:[10.5194/acp-10-10965-2010](https://doi.org/10.5194/acp-10-10965-2010)
9. Brasseur GP, Solomon S (2005) *Aeronomy of the middle atmosphere*, 3rd edn. Springer, The Netherlands

10. Carlotti M et al (2006) GMTR: two-dimensional geo-fit multitarget retrieval model for MIPAS/ENVISAT observations. *Appl Opt* 45:716–727
11. Christian HJ, Blakeslee RJ, Boccippio DJ, Boeck WL, Buechler DE, Driscoll KT, Goodman SJ, Hall JM, Koshak WJ, Mach DM, Stewart MF (2003) Global frequency and distribution of lightning as observed from space by the optical transient detector. *J Geophys Res* 108(D1):4005. doi:[10.1029/2002JD002347](https://doi.org/10.1029/2002JD002347)
12. Dinelli BM et al (2010) The MIPAS2D database of MIPAS measurements retrieved with a multi-target 2-dimensional tomographic approach. *Atmos Meas Tech* 3:355
13. Enell C-F et al (2008) Parameterisation of the chemical effect of sprites in the middle atmosphere. *Ann Geophys* 26:13–27
14. Gordillo-Vazquez F (2008) Air plasma kinetics under the influence of sprites. *J Phys D Appl Phys* 41(234):016
15. Hiraki Y et al (2008) Chemistry of sprite discharges through ion-neutral reactions *Atmos. Chem Phys* 8:3919–3928
16. Krehbiel PR, Riousset JA, Pasko VP, Thomas RJ, Rison W, Stanley MA, Edens HE (2008) Upward electrical discharges from thunderstorms. *Nature*. doi:[10.1038/ngo162](https://doi.org/10.1038/ngo162)
17. Marsh DR et al (2013) Climate change from 1850 to 2005 simulated in CESM1(WACCM). *J Clim* 26:7372–7391
18. Neubert T et al (2008) Recent results from studies of electrical discharges in the mesosphere. *Surv Geophys* 29:71
19. Pasko VP (2010) Recent advances in theory of transient luminous events. *J Geophys Res (Space Physics)* 115:00–35
20. Peterson H et al (2009) NO<sub>x</sub> production in laboratory discharges simulating blue jets and red sprites. *J Geophys Res* 114: A00E07
21. Rodger CJ, Seppala A, Clilverd MA (2008) Significance of transient luminous events to neutral chemistry: experimental measurements. *Geophys Res Lett* 35(AQ8):7803
22. Schumann U, Huntrieser H (2007) The global lightning-induced nitrogen oxides source. *Atmos Chem Phys* 7(14):3823–3907
23. Sentman DD et al (1995) Preliminary results from the Sprites94 aircraft campaign: 1 Red sprites. *Geophys Res Lett* 22:1205
24. Sentman DD et al (2008) Plasma chemistry of sprite streamers. *J Geophys Res* 113(11):112
25. Winkler H, Notholt J (2014) The chemistry of daytime sprite streamers—a model study. *Atmos Chem Phys* 14(7):3545–3556